Available online at www.sciencedirect.com
ScienceDirect
Applied Surface Science 253 (2006) 950–958
applied surface science
www.elsevier.com/locate/apsusc

Fundamental processes of aluminium corrosion studied under ultra high vacuum conditions

M. Frerichs, F. Voigts, W. Maus-Friedrichs *

Institut für Physik und Physikalische Technologien, Technische Universität Clausthal, Leibnizstraße 4, D-38678 Clausthal-Zellerfeld, Germany

Received 8 December 2005; received in revised form 18 January 2006; accepted 18 January 2006
Available online 23 February 2006

Abstract

Surface sensitive electron spectroscopy was applied to study the fundamental processes of aluminium corrosion. We used metastable induced electron spectroscopy (MIES) and ultraviolet photoelectron spectroscopy (UPS) for the investigation of the densities of states of surface and bulk, respectively. Furthermore we applied X-ray photoelectron spectroscopy (XPS) to investigate the chemical composition of the top surface layers. All measurements were performed under ultra high vacuum conditions.

Al films with thicknesses of 7 nm were investigated. Both the interaction of oxygen and water with these films leads to the formation of an aluminium–oxygen layer, which is partly composed of stoichiometric Al_2O_3. Weak heat treatment at 770 K transforms the surface layer into Al_2O_3 with a thickness of about 2 nm. Further gas offer does not lead to an increase of this thickness, neither for oxygen nor for water. Additional to the oxygen offer, water exposure leads to the formation of OH species in the top aluminium–oxygen layer to a small amount. Weak heat treatment to 770 K removes this species completely. Water exposure leads to a much faster oxide formation than oxygen exposure. We try to give a model for the fundamental corrosion processes on a molecular scale.

PACS: 68.43.−h; 73.20.At; 69.60.−i; 81.65.Mq

Keywords: Corrosion; Aluminium; Photoelectron spectroscopy (UPS, XPS); Metastable induced electron spectroscopy (MIES)

1. Introduction

Corrosion of aluminium has been studied extensively by means of electrochemical and other analytical methods commonly used in materials science. On aluminium surfaces, a passivating oxide film is formed immediately under atmospheric conditions as well as in pH-neutral liquids like water. Furthermore, in water this oxide is transformed into a passivating $Al(OH)_3$-film. See recent reviews for detailed information [1–3].

In technical applications, especially in light weight constructions, aluminium is alloyed typically with Mg, Zn, Cu or Fe. These alloys provide a strongly increased strength but decrease corrosion resistance significantly [1,2]. The naturally formed oxide films are thin, showing typical growth rates between 0.1 and 1 μm/year depending on their environment [3]. The interaction of oxygen and water with aluminium surfaces has been studied fundamentally previously. Theoretical calculations show the possible interaction processes between impinging oxygen and aluminium surfaces [4]. Others have used XPS to study the interaction of water and oxygen with aluminium after atmospheric exposure [5,6]. The initial stages of oxidation on aluminium have been studied by XPS and UPS [7–10].

Macroscopic observable corrosion depends on the interaction of single molecules (from the ambient atmosphere or liquids) with the very outermost surface layer. Therefore, a satisfying complete description of corrosion processes requires investigations with surface science techniques beginning under controlled vacuum conditions and ending up with realistic simulations of ambient atmospheres or liquids.

In this study we present results for the fundamental interaction of oxygen and water molecules with amorphous aluminium films, prepared under controlled conditions. Results for corrosion of these aluminium films studied under ambient

* Corresponding author.
E-mail address: w.maus-friedrichs@pe.tu-clausthal.de (W. Maus-Friedrichs).

0169-4332/$ – see front matter © 2006 Elsevier B.V. All rights reserved.
doi:10.1016/j.apsusc.2006.01.039

conditions will be presented in a forthcoming paper. Further studies will address the corrosion of Al alloys (AA7075), which are of recent interest (see for example [11]).

We apply various surface sensitive electron spectroscopic techniques capable of characterizing the atomic composition and chemical condition of the surface itself as well as yielding information on the top layers, which are responsible for the corrosion reactions.

2. Experimental

Measurements are carried out using an ultrahigh vacuum (UHV) apparatus with a base pressure of 5×10^{-9} Pa. The vacuum is produced by an ion getter pump (Perkin & Elmer) and a turbo-molecular pump (Varian V450A) and controlled by cold cathode gas discharge pressure sensors (Pfeiffer Vacuum Active Line). A quadrupole mass spectrometer (QMS, Balzers QMG 112) is used for analyzing the composition of the residual gas.

Electron spectroscopy is performed with a hemispherical analyzer (VSW HA 100) in combination with a He^*/HeI source for metastable induced electron spectroscopy (MIES) and ultraviolet photoelectron spectroscopy (UPS) as well as with a commercial non-monochromatic X-ray source (Specs RQ20/38C) for X-ray photoelectron spectroscopy (XPS).

During XPS, X-ray photons hit the surface under an angle of 80° to the surface normal, illuminating a spot with a diameter of some mm. Emitted electrons are analyzed by the hemispherical analyzer under 10° to the surface normal with a resolution of 1.1 eV. All XPS spectra are displayed as a function of the electron binding energy with respect to the Fermi level. XPS peaks are fitted mathematically using overlapping gauss profiles. The fitting is performed applying OriginPro7 (OriginLab Corporation) including the PFM add on. The peak positions and the full widths at half maximums (FWHMs) of the metallic Al 2p peak (denoted by Al_I in the following) and the O 1s peak for stoichiometric Al_2O_3 (denoted by O_I) were obtained from preliminary measurements (not shown here). For obtaining reliable fitting results these values (peak position and FWHM of Al_I and O_I) were used as parameters during the fitting procedure.

MIES and UPS are performed applying a cold cathode gas discharge via a two-stage pumping system. Here, metastable He atoms and HeI photons are produced. The ratio between He^* 2^3S and He^* 2^1S amounts to 7:1 [12]. The He^* 2^1S atoms are very effective converted into He^* 2^3S when approaching the surface of a metal [13]. Therefore, no contribution of the He 2^1S-surface interaction can be detected. A time-of-flight technique is used to separate electrons emitted by He^* (MIES) and HeI (UPS) interaction with the surface. The mixed He^*/HeI beam strikes the surface under an angle of 45° and illuminates an area of about 2 mm diameter on the sample surface. MIES and UPS spectra are simultaneously recorded by the hemispherical analyzer with a resolution of 220 meV under normal emission within 130 s.

Metastable He^* atoms may interact with the sample via different mechanisms depending on surface electronic structure and work function [14,15]. For the surfaces studied here only Auger deexcitation (AD) and Auger neutralization (AN) occur.

During AD an electron from the sample surface fills the 1s orbital of the impinging He^*. Simultaneously the He 2s electron is emitted carrying the excess energy. The resulting spectra directly display the surface density of states (SDOS). The excitation potential of the He^* amounts to 19.8 eV [14–17].

AN is a two-step process. Near the surface the He 2s electrons are resonantly transferred into unoccupied states of the sample surface. Subsequently, an electron from the surface fills He^+ 1s, simultaneously emitting another electron from the surface carrying the excess energy. The resulting spectra display a self-convolution of the SDOS [14,16,17].

Because the He^* atoms interact with the surface in distances typically between 0.3 and 0.5 nm in front of it, MIES is extremely surface sensitive and displays the SDOS of the uppermost layer of the sample only. To distinguish surface from bulk effects, AD-MIES and UPS can be compared directly.

All MIES and UPS spectra are displayed as a function of the electron binding energy with respect to the Fermi level. The surface work function can be determined from the left onset of the MIES or the UPS spectra with an accuracy of ±0.1 eV.

Aluminium films were produced by evaporating 99.999% pure Al (ChemPur GmbH) from a commercial metal evaporator (Omicron EFM3) at a flux of about 0.9 monolayers (ML) per minute in situ. One ML corresponds to one complete surface Al layer. These layers were produced on clean Si(1 0 0) at room temperature. The quality of these films was checked by MIES and XPS. Typical film thicknesses amount to 7 nm (= 17 ML) estimated by the attenuation of the Si 2s and Si 2p peaks in XPS after evaporating Al. Si substrates were used because of their easy handling and their availability. The amorphous films obtained on Si are more useful for the simulation of technical aluminium than usual single crystals. H_2O and O_2, respectively, are offered by backfilling the chamber via a controlled leak valve. Several pump–freeze cycles were done for cleaning the water. The gas inlet system, pumped by an oil free membrane pump (Ilm-vac MP201 T) and a cryo pump, is baked out for 24 h before each experiment. The cleanness of the O_2 as well as the H_2O is checked by QMS.

3. Results

Fig. 1 shows MIES (a) and UPS (b) spectra of a thick aluminium film (7 nm), which was prepared on a Si(1 0 0) sample as described above. The bottom spectra displayed are due to the pure Al film, respectively. MIES and UPS spectra being collected continuously with increasing oxygen offer are displayed in a waterfall manner. The oxygen exposure is given on the right side of the spectra, respectively.

During oxygen exposure a distinct peak develops at $E_B = 7.3$ eV in MIES and 7.0 eV in UPS. These peaks are typical for the interaction of oxygen with metallic surfaces and

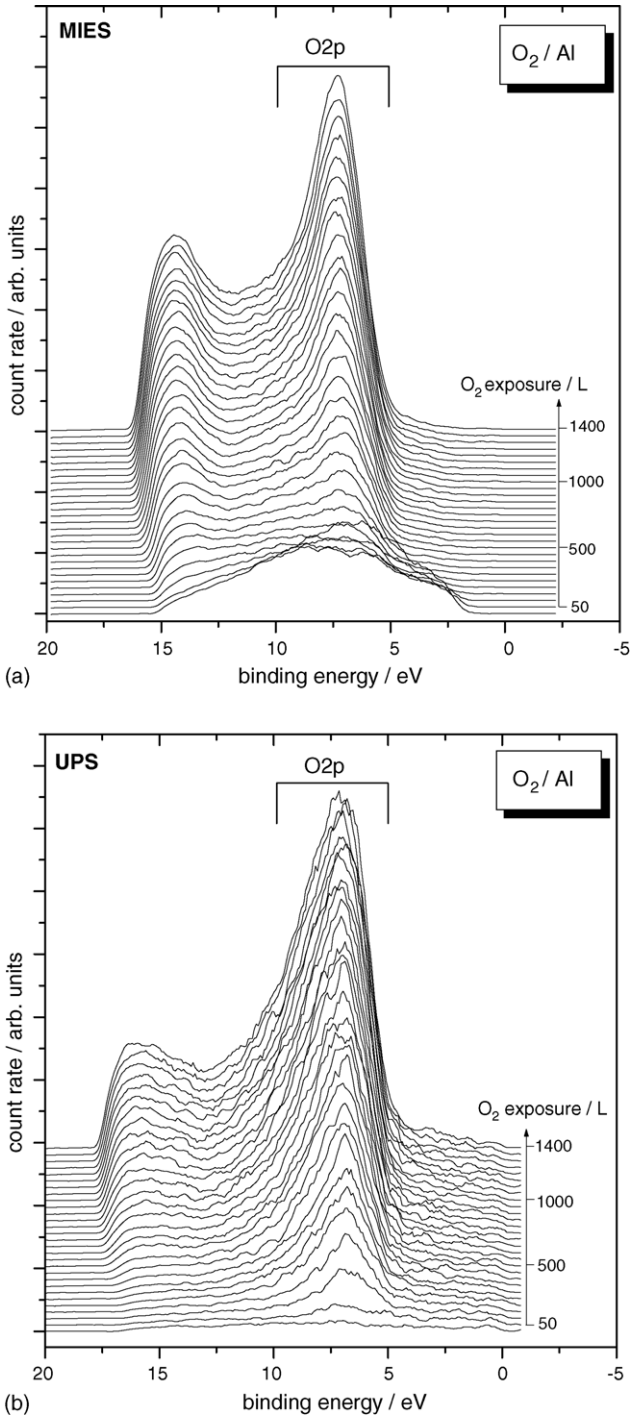

Fig. 1. MIES (a) and UPS (b) spectra of an aluminium film (thickness 7 nm) displayed as a function of oxygen exposure. Exposures are given with the spectra on the right side. See text for a detailed description.

are due to ionization from the oxygen O 2p orbital. Comparable MIES and UPS results for Al_2O_3 have been published previously [7,18,19]. The peaks at the high binding energy cut-off are due to secondary electrons and will not be discussed further. During the oxygen offer, the work function of the sample decreases from 4.4 eV for the clean Al to 3.3 eV after 1400 L of O_2, which corresponds well to the values published by Kravchuk et al. [7] for the initial stages of oxidation of an Al(1 0 0) single crystal. The development of the work function during oxygen and water exposure will be discussed in detail with Fig. 6.

The bottom MIES spectrum, corresponding to the pure Al film, is induced by the Auger neutralization process and therefore displays a self-convolution of the SDOS. With increasing oxygen exposure a change of the interaction process occurs. The top spectra are due to the Auger Deexcitation process, which directly reflects the SDOS. The bottom UPS spectrum is very weak, because the interaction of HeI photons with the Al valence-orbitals is very inefficient [20–22]. The intensity of the spectra increases with the appearance of the peaks due to the oxygen 2p orbitals.

The MIES and UPS spectra of the oxygen saturated Al films do not correspond to stoichiometric Al_2O_3 [7,19,23]. This requires a mild heating procedure, which will be shown in Fig. 4.

Fig. 2 shows XPS results of the aluminium surface exposed to 1400 L of oxygen, which corresponds to the top spectra of Fig. 1. Fig. 2(a and b) show the Al 2p emission and the O 1s emission of this surface, respectively. Fig. 2(c and d) show results for the same surfaces after heating to 770 K for 400 s.

The Al 2p and O 1s features consist of several contributions induced by the different chemical environments of the Al or O atoms. These contributions can be represented by a number of Gaussian type functions, because the form of the peak is determined by the Gaussian type transmission function of the hemispherical analyzer [24]. We applied computer controlled Gaussian fits to the XPS spectra, allowing us to distinguish the different contributions. The spectral underground was substracted linearly. This procedure delivers the peak positions, the full widths at half maximums (FWHMs) and the relative intensities of the different contributions.

The Al 2p peak consists of two contributions from unoxidized metallic Al^0 (denoted by Al_I in Fig. 2) at $E_B = 74.59$ eV with a FWHM of 1.61 eV and from oxidized Al^{3+} denoted by Al_{II} at $E_B = 76.48$ eV with a FWHM of 3.77 eV. The O 1s peak also consists of two contributions, O_I at $E_B = 533.46$ eV and O_{II} at $E_B = 535.71$ eV, before heating to 770 K. After heat treatment, O_{II} disappears and O_I is found at $E_B = 533.85$ eV. Al_{II} shifts slightly to higher binding energy ($E_B = 76.69$ eV) and the relative intensity is getting marginally higher. All peak positions and FWHMs are summarized in Table 1. Peak positions and FWHMs correspond well to published data [5–7,10]. Further XPS measurements (not shown here) show Al_{II} and O_I at the same binding energies for bulk Al_2O_3 material. The XPS spectra do not show any contribution from the silicon substrate, which means that the Al/Al-oxide film is closed. The results will be discussed in detail in Section 4.

Fig. 3 shows MIES (a) and UPS (b) results of the aluminium film exposed to water. During the exposure, peaks at $E_B = 7.7$ eV in MIES and $E_B = 7.3$ eV in UPS develop, which are comparable with the O_2 interaction already discussed above. A second peak develops after exposure of about 500 L H_2O at $E_B = 12.0$ eV in MIES and $E_B = 13.5$ eV in UPS showing less intensity than the O 2p peak. Fig. 3(c) shows the

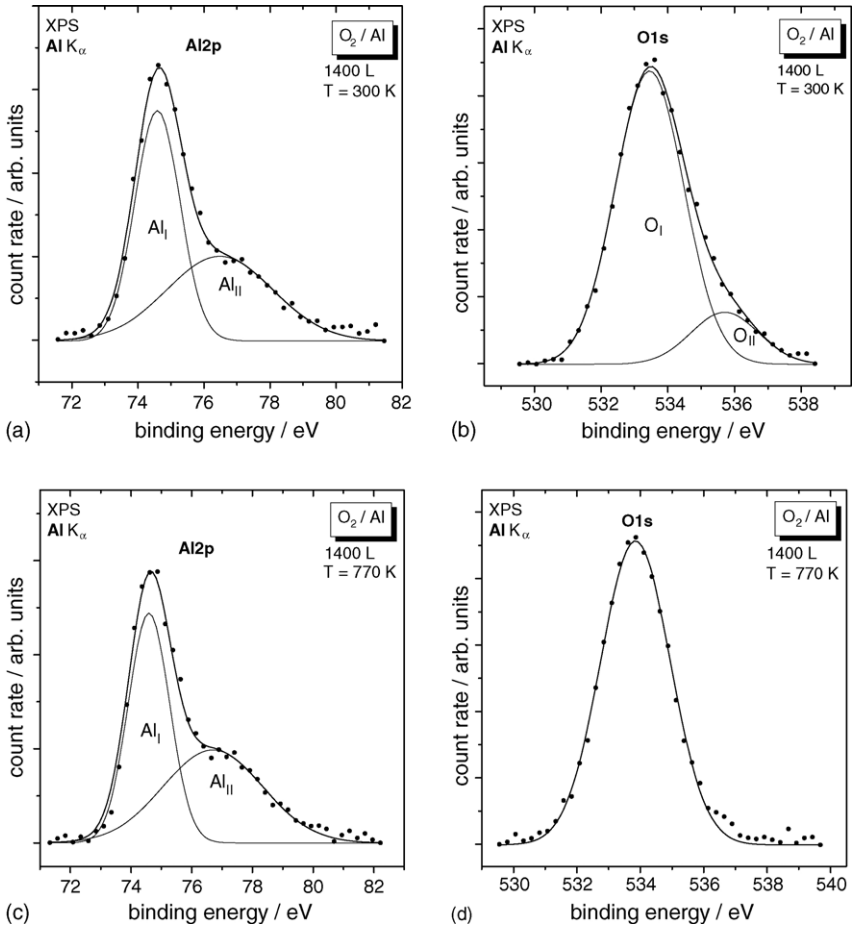

Fig. 2. XPS spectra of the oxidized aluminium (1400 L O_2) without heat treatment (a and b) and after heating to 770 K (c and d). Shown are the Al 2p (a and c) and the O 1s (b and d) ranges, respectively. See text for a detailed description.

MIES spectra after exposure of 1400 L O_2 and after exposure of 1200 L H_2O. The third graph shows the difference between these two spectra. Two peaks are observable at 8.4 and 11.9 eV. The distance and ratio of these two peaks are known and belong to the interaction of the He^* with adsorbed OH^- groups [25,26]. A detailed discussion will follow in Section 4. The work function of the sample decreases drastically with increasing water exposure. After an exposure to 200 L it reaches 2.8 eV; the saturation value of 2.6 eV is reached after an exposure to 1200 L.

Fig. 4 shows results from the heat treatment of the water-saturated Al sample from Fig. 3. The uppermost spectra of Figs. 3 and 4 correspond to each other, respectively. The sample was heated in situ in steps from about 20 K finally reaching a temperature of 770 K in the bottom spectra. The spectra at 770 K correspond well to the spectra of Al_2O_3 not shown here with the exception of the small contributions beyond the O 2p valence band maximum. These contributions are most likely due to metallic Al from the segregation of Al atoms to the surface during heat treatment.

The first spectra accordingly show the same two peaks as in Fig. 3. With increasing temperature, the OH peaks vanish at around 590 K. The FWHM of the O 2p peak widens during the heat treatment. This behavior has been observed before on oxygen saturated Al [7]. These effects are much more obvious

Table 1
Summarized values from Fig. 2 (O_2/Al)

Feature	Temperature (K)	Peak	Peak position (eV)	FWHM (eV)	Relative intensity
Al 2p	300	Al_I	74.59	1.61	0.538 (= I_m)
		Al_{II}	76.48	3.77	0.462 (= I_{mo})
O 1s	300	O_I	533.46	2.42	0.852
		O_{II}	535.71	2.38	0.148
Al 2p	770	Al_I	74.59	1.61	0.508
		Al_{II}	76.69	3.87	0.492
O 1s	770	O_I	533.85	2.58	1.0

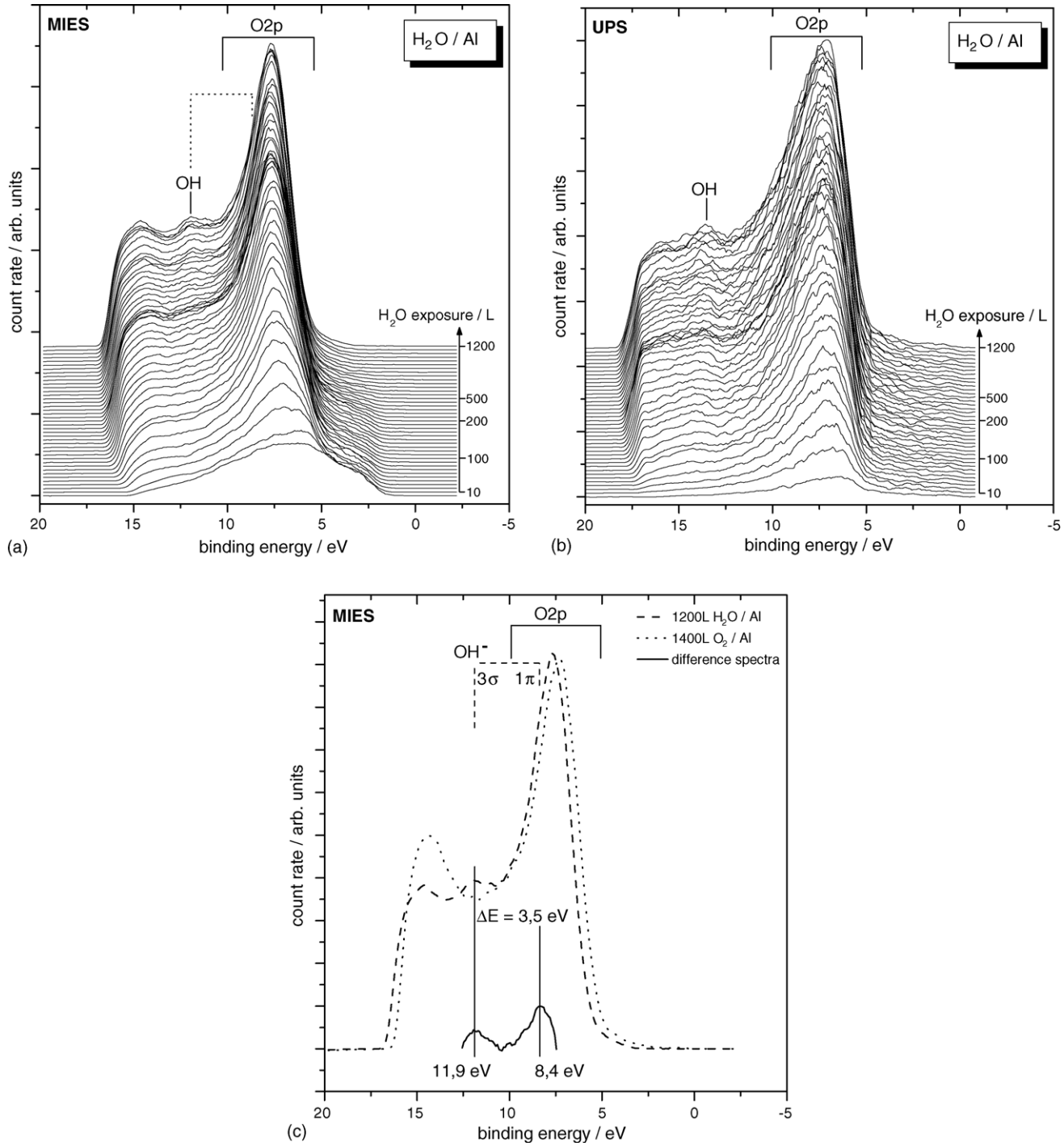

Fig. 3. MIES (a) and UPS (b) spectra of an aluminium film (thickness 7 nm) displayed as a function of water exposure. Exposures are given with the spectra on the right side. (c) Shows the top spectra from Figs. 1(a) and 3(a) and their difference spectrum. See text for a detailed description.

in MIES. The work function of the sample rises during the heat treatment up to 3.3 eV at 770 K.

Fig. 5 shows XPS measurements of the aluminium surface exposed to 1400 L of water. The O_I- and O_{II}-peaks correspond to the peaks from Fig. 2 (see Table 1).

The sample was heated to different temperatures up to 770 K, respectively. O_{II} disappears at 770 K as was already observed during the heat treatment of the oxygen exposed Al films. All peak positions and FWHMs are summarized in Table 2.

Fig. 6 compares the integral emission from the O 2p orbital as derived from UPS and the work function during oxygen exposure from Fig. 1(b) (displayed as dots) and during water exposure (displayed as triangles), respectively. Additionally, the work function after annealing to 770 K both for O_2 and H_2O exposure is shown. The results will be discussed in Section 4. Annealing to 770 K was also done for lower gas exposures resulting in the same work functions both for water and oxygen exposure, respectively.

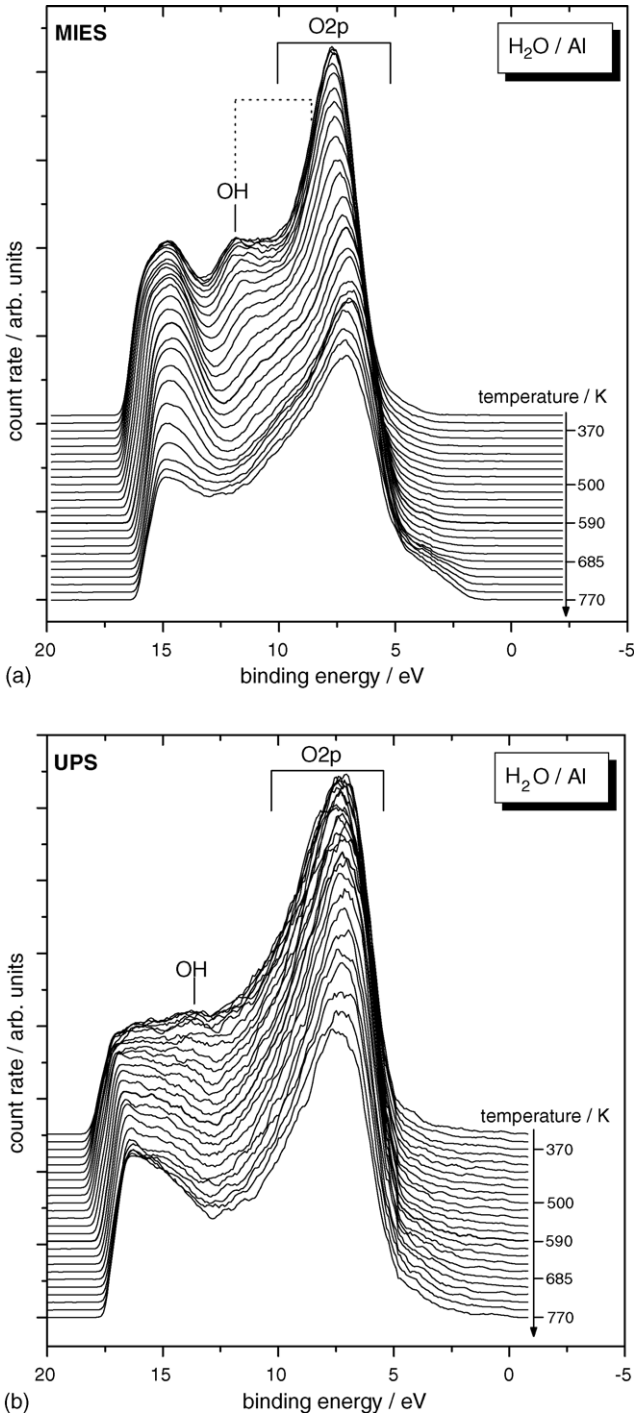

Fig. 4. MIES (a) and UPS (b) spectra of the water saturated aluminium (1200 L H_2O) as a function of surface temperature. Temperatures are given with the spectra on the right side. See text for a detailed description.

4. Discussion

Oxygen molecules approaching the aluminium surface have three possibilities for interacting with the surface. Either they are dissociated in the vicinity of the surface by a charge transfer into the oxygen antibonding molecular orbital or otherwise the whole oxygen molecule is reflected from the surface [4,27]. In the case of dissociation both oxygen atoms can adsorb on the surface (dissociative adsorption) or only one atom adsorbs on the surface, the other one exchanges as an O^- or O back to the gas phase (abstractive dissociation) [4]. After dissociation the adsorbed oxygen atoms are subsequently incorporated into the metallic layer. Fig. 1 shows this very clearly as O 2p formation. Nevertheless, XPS shows that only about 80% of these oxygen atoms are incorporated as stoichiometric oxide Al_2O_3, visible as O_I in Fig. 2 (see Table 1). The other oxygen atoms, denoted by O_{II}, appear to be incorporated into the composed Al/Al_2O_3 film but not being chemisorbed as oxide [9]. Heating to 770 K results in the transformation of O_{II} into O_I. No oxygen loss occurs as can be seen from the unchanged integral O 1s intensity. This means, that all oxygen atoms chemisorb in stoichiometric Al_2O_3 after heating as can be seen in Fig. 2(d). The position and relative intensities of Al_{II} and O_I correspond very well to the ones for bulk Al_2O_3 [28,29].

The Al_2O_3 layer thickness d on the Al film is calculated from the XPS peak intensities of Al_{II} (denoted by I_{mo}) and of Al_I (denoted by I_m) in the following manner [5,6]:

$$d = \lambda_{mo} \cos\theta \ln\left[\left(\frac{D_m \lambda_m}{D_{mo} \lambda_{ml}}\right)\left(\frac{I_{mo}}{I_m}\right) + 1\right] \quad (1)$$

where D_{mo} (6.024×10^{22} atoms cm^{-3} [5]) and D_m (4.605×10^{22} atoms cm^{-3} [5]) are the atomic densities of metal atoms in the oxide film and in the underlaying metal substrate, respectively, λ_{mo} (2.679 nm [30]) and λ_m (2.579 nm [30]) are the corresponding inelastic mean free paths of the electrons, and θ (10°) is the angle between surface normal and direction of emitted electrons. With the given values we obtain d = 2.1 nm as oxide layer thickness. This Al_2O_3 layer on top of the Al film provides a thickness, which may not be increased under the chosen conditions, independent of the amount of oxygen offered additionally. This means, that the Al film reaches a natural oxide thickness limit of 2.1 nm under the applied conditions. At this oxide thickness the MIES spectra show a clear band gap between the Fermi level at E_B = 0 eV and E_B = 4 eV. Therefore, further impinging oxygen molecules cannot interact with the surface via electron transfer into its antibonding molecular orbital. So the oxygen layer thickness limitation is caused by the missing oxygen molecule dissociation probability. Under real conditions, where for example aerosol particles are present, dissociation is possible, so further oxygen atom incorporation does take place [3].

The interaction of water with the aluminium films shows quite similar MIES and UPS spectra (Fig. 3) as seen during oxygen offer: a strong O 2p emission is observed with increasing exposure. This means that the impinging water molecules are completely dissociated, thus forming an oxide layer similar as during oxygen exposure. The XPS spectra of the O 1s peak (Fig. 5) showing at 300 and 770 K the same features than during oxygen exposure (Fig. 2) support this picture. After about 500 L H_2O exposure in MIES a second peak is developing at E_B = 12 eV. Fig. 3(c) shows the difference spectrum between water and oxygen exposure. In this

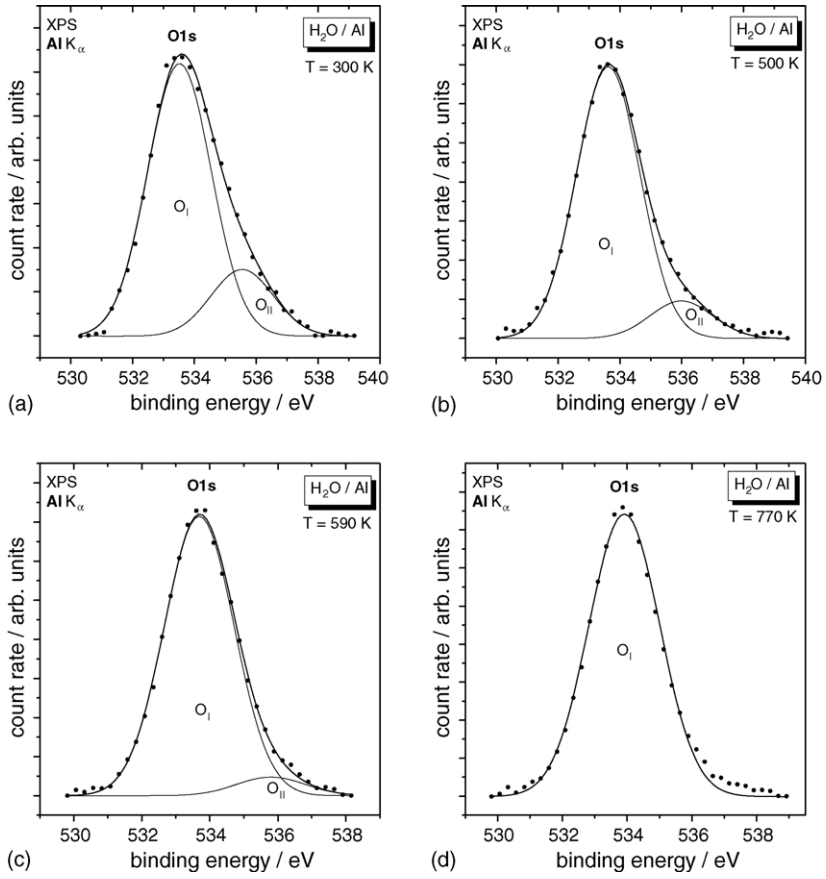

Fig. 5. XPS spectra of the water saturated Al surface (1500 L H_2O) after heat treatment to different temperatures. Shown is the O 1s range, respectively. See text for a detailed description.

difference spectrum two peaks are observable with a distance of 3.5 eV and a peak ratio of 3:1. From the literature it is well known that this two peaks descend from the interaction of the He^* with OH^- groups on top of the surface [25,26]. As the peak intensity of OH^- is about 10% of the O 2p peak and is not increasing even after higher water exposure (under UHV conditions) we suggest that OH only adsorbs at defect sites.

In UPS also a peak appears after about 500 L of water exposure, but at $E_B = 13.5$ eV. This peak is not as easy to explain as the one seen in the MIES spectra. It cannot be induced by surface adsorbed OH^- groups for two reasons: first, an interaction process leading to a peak shifting of 1.5 eV is not known. Second, the peak at $E_B = 13.5$ eV again amounts to about 10% of the O 2p peak. But as MIES is much more surface sensitive, in UPS an OH (surface) peak would be much smaller and most likely not visible. Additionally, a difference spectrum of the two UPS spectra after 1200 L water exposure and 1400 L oxygen exposure shows only the peak at $E_B = 13.5$ eV and not the second one of the usual OH^- doublet. Also, this peak cannot descend from any surface contamination, because XPS shows only the oxygen and aluminium related peaks, in particular the presence of carbon can be excluded. It is known that hydrogen adsorption on Al only takes place below a temperature of 190 K [8] and as the 13.5 eV peak disappears at the same temperature (590 K) as the OH^- peak in MIES (Fig. 4) we assume that the origin of the peak are OH molecules, but not on top of the

Table 2
Summarized values from Fig. 5 (H_2O/Al)

Feature	Temperature (K)	Peak	Peak position (eV)	FWHM (eV)	Relative intensity
O 1s	300	O_I	533.52	2.42	0.806
		O_{II}	535.55	2.38	0.194
O 1s	500	O_I	533.62	2.42	0.881
		O_{II}	535.9	2.38	0.119
O 1s	590	O_I	533.67	2.42	0.939
		O_{II}	535.8	2.38	0.061
O 1s	770	O_I	533.91	2.58	1.0

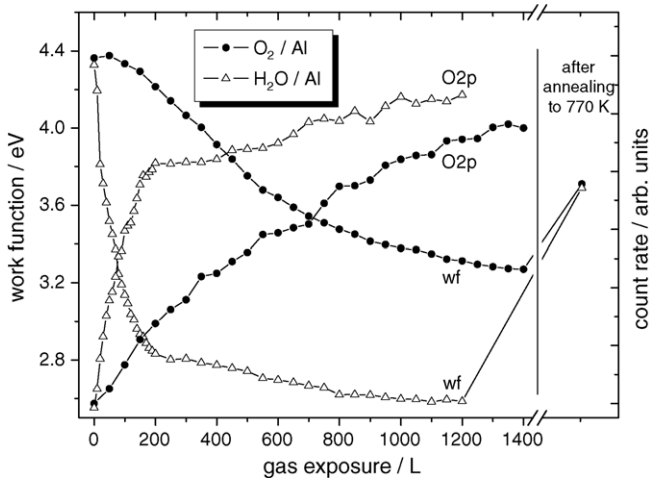

Fig. 6. Work function and O 2p (UPS) emission during oxygen and water exposure of the Al film as a function of the respective gas exposure. See text for a detailed description.

surface. The OH molecules may be incorporated into the aluminium oxide bulk. The peak shift of 1.5 eV may be possible due to the different chemical environment.

The thickness of the oxide film amounts to 1.9 nm after water saturation (1200 L) as has been calculated from Eq. (1).

The XPS spectra of Fig. 5 combined with Fig. 2 show an interesting aspect looking at the O_{II} peak. Usually, XPS spectra recorded after oxidation or hydroxylation [5,6] show a feature similar to the ones displayed in Figs. 2 and 5: the O 1s peak has a broadened side at higher binding energies. This broadening has been interpreted to be induced by OH, H_2O, C–O or O–C=O in the literature. As most work groups use atmospheric oxidation [5,6] on Al single crystal or technical Al alloys the presence of carbon, water or OH is very likely. However, in our work we can ensure the cleanness of the measurements and the gas exposure by QMS, MIES and UPS. The presence of carbon containing molecules can be excluded. Furthermore, MIES shows only a 10% OH contribution (but no H_2O) on top of the surface. This contribution is too small to be clearly discernable in UPS. Thus, no OH contribution to the O 1s peak can be seen in XPS, because XPS is even less surface sensitive than UPS. Kravchuk et al. [7] suggest in their work a three-step oxidizing process that leads to a stabilized, stoichiometric Al_2O_3 only after heating. Therefore we assume the feature O_{II} to descend from less coordinated oxygen incorporated into the metallic Al matrix and oxygen chemisorbed to the surface.

Further analysis of the spectra in Figs. 1 and 3 leads to the data in Fig. 6. It is a common method to study the reaction rate by analyzing the work functions of the reactive surfaces and their prominent peak integral intensities. In this case, the increase of the O 2p peak and the decrease of the work function is much faster during water exposure compared to oxygen exposure. During water exposure, the O 2p integral emission reaches 80% of its saturation value at an exposure of 200 L, while the same value is reached at 850 L during oxygen exposure. A similar tendency is observed for the work functions.

The saturation work function of the water exposed Al film is much lower due to OH groups at the surface, as has been discussed previously. Annealing to 770 K leads to the work function of Al_2O_3 both for water and oxygen exposure as shown in Fig. 6. This gives further support for the proposed Al_2O_3 formation.

5. Summary

Impinging oxygen molecules are dissociated in the vicinity of the Al surface. The oxygen atoms are adsorbed on the surface and are subsequently incorporated in the sub surface region of the Al film forming an amorphous oxide layer. Mild annealing to 770 K leads to the transformation into a completely stoichiometric Al_2O_3 film with a thickness of 2.1 nm. Further oxygen does not interact with the surface, because dissociation cannot take place any longer due to the missing electron density below the Fermi level. Under clean conditions, this aluminium oxide film is stable and prevents further corrosion of the material.

Impinging water molecules are completely dissociated near the surface of the Al film. Again, the oxygen atoms form an amorphous oxide layer. As soon as the surface begins to develop oxidic properties, complete dissociation of the H_2O becomes less likely and products of partly dissociation may adsorb on the surface. Thus, OH groups may be found at the surface in this stage of the experiment. Mild annealing to 590 K removes the OH groups from the surface, further annealing to 770 K leads to the formation of Al_2O_3 as described above, with a thickness of 1.9 nm. The corrosion rate during water exposure is significantly higher than during oxygen exposure, although both result in an oxide layer with a thickness of about 2 nm. On a molecular scale aluminium corrosion means oxide formation, self-inhibiting at a thickness of 2 nm, which corresponds to about four monolayers. The formation of OH groups to a small amount does not influence oxide thickness but probably the reaction velocity.

Acknowledgments

Financial support from the German Stiftung Industrieforschung (under contract no. S626) is gratefully acknowledged. The authors appreciate useful scientific discussions with Dipl.-Ing. S. Hollunder of the Institut für Maschinelle Anlagentechnik und Betriebsfestigkeit, Technische Universität Clausthal.

References

[1] H. Kaesche, Corrosion of metals, Springer Verlag, Berlin, 2003.
[2] K.-H. Tostman, Korrosion, Wiley-VCH, Weinheim, 2000.
[3] C. Leygraf, T.F. Graedel, Atmospheric corrosion, in: Electrochemical Society Series, Wiley-Interscience, New York, 2000.
[4] G. Katz, R. Kosloff, Y. Zeiri, J. Chem. Phys. 120 (8) (2004) 3931–3948.
[5] E. McCafferty, J.P. Wightman, Surf. Int. Anal. 26 (1998) 549–564.
[6] B.R. Strohmeier, Surf. Int. Anal. 15 (1990) 51–56.
[7] T. Kravchuk, R. Akhvlediani, V.V. Gridin, A. Hoffmann, Surf. Sci. 562 (2004) 83–91.
[8] S.A. Flodström, L.-G. Petersson, S.B.M. Hagström, J. Vac. Sci. Technol. 13 (1) (1976) 280–282.

[9] S.A. Flodström, R.Z. Bachrach, R.S. Bauer, S.B.M. Hagström, Phys. Rev. Lett. 37 (19) (1976) 1282–1285.
[10] M. Frerichs, F. Voigts, V. Kempter, G. Borchardt, W. Maus-Friedrichs, S. Hollunder, R. Masendorf, A. Esderts, Appl. Surf. Sci. 252 (2005) 108–112.
[11] Q. Meng, G.S. Frankel, Corrosion 60 (2004) 897–905.
[12] J. Günster, Ph.D. Thesis, Technische Universität Clausthal, 1996.
[13] B. Woratschek, W. Sesselmann, J. Küppers, G. Ertl, H. Haberland, Phys. Rev. Lett. 55 (1985) 611.
[14] Y. Harada, S. Masuda, H. Ozaki, Chem. Rev. 97 (1997) 1897–1952.
[15] H. Morgner, Adv. Atom. Mol. Opt. Phys. 42 (2000) 387–488.
[16] G. Ertl, J. Küppers, Low Energy Electrons and Surface Chemistry, VCH, Weinheim, 1985.
[17] V. Kempter, Mater. Sci. Forum 239–241 (1997) 621–628.
[18] A. Hitzke, J. Günster, J. Kolaczkiewicz, V. Kempter, Surf. Sci. 318 (1994) 139–150.
[19] J. Günster, M. Brause, Th. Mayer, A. Hitzke, V. Kempter, Nucl. Instrum. Methods B 100 (1995) 411–416.
[20] D. Ochs, W. Maus-Friedrichs, M. Brause, J. Günster, V. Kempter, V. Puchin, A. Shluger, L. Kantorovich, Surf. Sci. 365 (1996) 557–571.
[21] W.C. Price, in: C.R. Brundle, A.D. Baker (Eds.), Electron Spectroscopy: Theory, Techniques and Applications, vol. I, Academic Press, London, 1977.
[22] W. Eberhardt, F.J. Himpsel, Phys. Rev. Lett. 42 (20) (1979) 1375–1378.
[23] V.E. Henrich, P.A. Cox, The Surface Science of Metal Oxides, Cambridge University Press, Cambridge, 1994.
[24] D. Briggs, J.T. Grant, Surface Analysis by Auger and X-ray Photoelectron Spectroscopy, IM Publications and Surface Spectra Limited, Manchester, 2003.
[25] W. Maus-Friedrichs, A. Gunhold, M. Frerichs, V. Kempter, Surf. Sci. 488 (2001) 239–248.
[26] P.A. Thiel, T.E. Madey, Surf. Sci. Rep. 7 (1987) 211.
[27] K. Wandelt, Surf. Sci. Rep. 2 (1982) 1–121.
[28] C.D. Wagner, W.M. Riggs, Handbook of X-Ray Photoelectron Spectroscopy, Perkin-Elmer, Eden Prairie, 1979.
[29] M. Frerichs, Ph.D. Thesis, Technische Universität Clausthal, to be published.
[30] NIST Inelastic Mean Free Path Database 1.1, http://www.nist.gov/srd/nist71.htm.